AIP Journal of Applied Physics

Rolling motion of an elastic cylinder induced by elastic strain gradients

Lei Chen and Shaohua Chen

Citation: Journal of Applied Physics **116**, 164701 (2014); doi: 10.1063/1.4900614
View online: http://dx.doi.org/10.1063/1.4900614
View Table of Contents: http://scitation.aip.org/content/aip/journal/jap/116/16?ver=pdfcov
Published by the AIP Publishing

JOURNAL OF APPLIED PHYSICS **116**, 164701 (2014)

Rolling motion of an elastic cylinder induced by elastic strain gradients

Lei Chen and Shaohua Chen[a)]
LNM, Institute of Mechanics, Chinese Academy of Sciences, Beijing 100190, China

(Received 1 September 2014; accepted 17 October 2014; published online 30 October 2014)

Recent experiment shows that an elastic strain gradient field can be utilized to transport spherical particles on a stretchable substrate by rolling, inspired by which a generalized plane-strain Johnson-Kendall-Roberts model is developed in this paper in order to verify possible rolling of an elastic cylinder adhering on an elastic substrate subject to a strain gradient. With the help of contact mechanics, closed form solutions of interface tractions, stress intensity factors, and corresponding energy release rates in the plane-strain contact model are obtained, based on which a possible rolling motion of an elastic cylinder induced by strain gradients is found and the criterion for the initiation of rolling is established. The theoretical prediction is consistent well with the existing experimental observation. The result should be helpful for understanding biological transport mechanisms through muscle contractions and the design of transport systems with strain gradient.
 [http://dx.doi.org/10.1063/1.4900614]

I. INTRODUCTION

The JKR (Johnson-Kendall-Roberts), DMT (Derjaguin-Muller-Toporov), and MD (Maugis-Dugdale) models,[1–3] as three representative and pioneering work in the field of adhesive contact mechanics have been extensively developed in recent years. In the JKR model,[1] an equilibrium contact area is established via Griffith energy balance between elastic energy and surface energy, which results in compressive stress in the central region of contact and crack-like singular tensile stress near the edge of contact; the contact area remains finite until a critical pull-off force is reached. In the DMT model,[2] molecular forces outside the Hertz contact area are considered, but these forces are assumed not to change the contact profile of the Hertz solution. It was later realized by Tabor[4] that the JKR model is more suitable for contact between relatively large and soft bodies, while the DMT model is more suitable for contact between small and rigid bodies. In 1992, Maugis[3] developed a unified model linking the JKR and DMT models by extending the Dugdale model to the case of adhesive contact between two elastic spheres. Due to its specific application range, JKR model has been adopted to explain many interesting biological phenomena, such as gecko adhesion,[5–7] cell-cell adhesion,[8] cells on stretched substrates.[9,10]

The mechanisms of cell-cell and cell-substrate adhesion are related with many fields of biology, including embryonic development, cancer metastasis, cellular transport, endo- and exocytosis, tissue and cellular engineering.[11–13] It is widely believed that cells can sense and respond to mechanical forces from extracellular environments[14–17] through surface or interface adhesion. As a result, they could detach, slip, or roll on a substrate in response to these forces.[18–25]

In such biological systems, another ubiquitous phenomenon is transport via tissue contraction. As a prominent example, smooth muscle contraction is essential for oosperm transport from ovary to uterus through the fallopian tube during pregnancy,[26,27] the whole transport process is a dynamic, micro-scale and cross-disciplinary problem. In addition, specific adhesion molecules, such as $\alpha3$, $\beta1$, αV, $\alpha2\beta1$, have been found experimentally in fallopian tube, as well as fibronectin, an extracellular adhesive glycoprotein that mediates cell-matrix adhesion experiment.[28,29] All these adhesive integrins were proved experimentally to play a significant role for oosperm-oviduct bonding.[28] Though it is clear that the transport of oosperm involves smooth muscle contraction, the detailed mechanism still remains elusive,[26,27,30–34] due in part to the complexity of cell-substrate interactions via receptor-ligand binding as well as various physical forces inside and outside the cytoskeleton.[14,15,35–37]

In order to disclose the mechanical mechanism of oosperm transport induced by smooth muscle contraction, a recently biomimetic experiment suggests that an elastic strain gradient can be utilized to transport spherical particles on a stretchable substrate by rolling.[38] In the experiment, a sticky elastic layer made of thermal plastic rubber is put on a rigid epoxy resin substrate and an interfacial crack is introduced near the edge of the interface, meanwhile a horizontal displacement is imposed at the detached end of the elastic layer. As the layer is stretched beyond a critical strain, the interfacial crack starts to propagate, inducing an elastic strain gradient in the layer that moves with the crack tip. A latex bubble is slightly put on the sticky elastic layer ahead of the interfacial crack tip, and a free adhesive contact area is formed due to the interface interaction. As the moving crack with an elastic strain gradient field ahead of its tip reaches the position that the bubble adheres, the elastic bubble begins to roll along the surface. Based on the work of a 3D pressurized spherical bubble in adhesive contact with a stress-free substrate,[39] a simple 3D model of a pressurized spherical bubble adhering on an elastic substrate subject to a strain gradient has been established. Both experiment and the simple theoretical model indicate that not only the strain gradient η but also the average strain in substrates influences the initiation of rolling

a)Author to whom correspondence should be addressed. Electronic mail: chenshaohua72@hotmail.com

of the spherical particle, while the steady state rolling of the spherical particle depends on the strain gradient. Either the initiation of rolling or the steady state rolling is also related with the contact radius a and the inherent membrane strain ε_0 of the elastic bubble.[38] It provides some enlighten thoughts that asymmetric strain fields generated by smooth muscle contractions may drive the oosperm rolling along the fallopian tube. A comparable finding to the present rolling motion induced by the inhomogeneous strain field is the spontaneous migration of droplets resulted from an asymmetrical chemical interaction.[40–44] Furthermore, temperature gradient was also found as a driving force that could move a bubble against liquid flow.[45] All the interesting phenomena indicate that the heterogeneity of environmental fields can be a generally driving force for transport.

Inspired by the above rolling mechanism predicted experimentally and theoretically, it is reasonable to infer that an elastic cylinder can also roll on an elastic substrate subject to a graded strain. What factors will influence the rolling of cylinders induced by strain gradient in substrates? What difference may exist between the elastic cylinder rolling case and the elastic spherical bubble rolling one?

II. THEORETICAL MODEL AND ANALYSIS

A two-dimensional model is established in order to answer the above questions, where an elastic cylinder adheres on an elastic substrate subject to a strain gradient as shown in Fig. 1. According to the rolling experiment,[38] an assumption of perfect adhesion without slipping between the elastic cylinder and the stretched substrate is adopted in this model. A Cartesian coordinate system (x, y) is placed at the contact region. For such a cylinder in adhesive contact with an initially stress-free substrate via Van der Waals interaction, the contact region is symmetric with a half contact width as shown in Fig. 1(a)[9,46,47]

$$a_0 = [32R^2\Delta\gamma/(\pi E^*)]^{1/3}, \tag{1}$$

where R is the radius of the above cylinder, $\Delta\gamma$ is the work of adhesion of the contact interface, and E^* is an effective Young's modulus, $\frac{1}{E^*} = \frac{1-\nu_1^2}{E_1} + \frac{1-\nu_2^2}{E_2}$, E_j and ν_j $(j = 1, 2)$ being the Young's modulus and Poisson's ratio of the cylinder $(j = 1)$ or substrate $(j = 2)$.

After the substrate is subjected to a non-uniform strain field $\varepsilon(x)$, the contact region becomes asymmetric, occupying the region $-b \le x \le a$, as shown in Fig. 1(b). With the help of contact mechanics,[48] the continuity of displacements across the contact interface requires

$$\begin{cases} \bar{u}_{x1} - \bar{u}_{x2} = \displaystyle\int_0^x \varepsilon(t)\mathrm{d}t \\ \bar{u}_{y1} - \bar{u}_{y2} = \delta - \dfrac{x^2}{2R} \end{cases} -b \le x \le a, \tag{2}$$

where $\bar{u}_{xj}$ $(\bar{u}_{yj})$ denotes the displacement in the x (y) direction of the cylinder $(j = 1)$ or substrate $(j = 2)$, δ is the displacement at the center of the cylinder,[48] and $x^2/(2R)$ is due to a parabolic approximation of the cylinder profile, usually adopted in contact mechanics.[48] Note that the lower bound

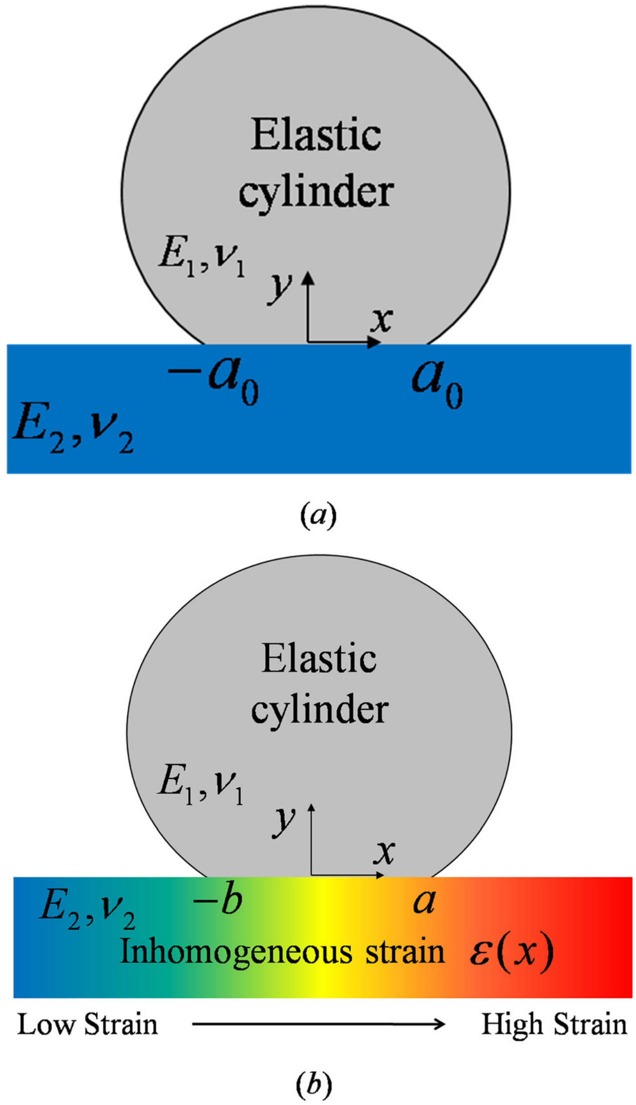

FIG. 1. A two-dimensionally adhesive contact model of an elastic cylinder in adhesive contact with an elastic substrate. (a) The substrate is stress-free and the width of contact region is $2a_0$. (b) The substrate is subjected to a graded strain, which induces an asymmetric width of contact region $-b \le x \le a$.

of the integral in Eq. (2) can be arbitrarily chosen without affecting the stress field.

Following similar notations used in our previous study of a cylinder adhering on a stretched substrate,[9] the surface displacements of an elastic half-space can be related to the surface tractions $P(x)$ and $Q(x)$ via Green's functions of an elastic half-space. Thus, the governing equations of tractions and displacements along the cylinder-substrate interface can be written as

$$\begin{cases} \dfrac{1}{\pi}\displaystyle\int_{-b}^{a} \dfrac{Q(s)}{s-x}ds - \beta P(x) = \dfrac{1}{2}E^*\varepsilon(x) \\ \dfrac{1}{\pi}\displaystyle\int_{-b}^{a} \dfrac{P(s)}{s-x}ds + \beta Q(x) = -\dfrac{1}{2}E^*\dfrac{x}{R}, \end{cases} \tag{3}$$

where $\beta = \frac{1}{2}\frac{(1-2\nu_1)(1+\nu_1)/E_1 - (1-2\nu_2)(1+\nu_2)/E_2}{(1-\nu_1)(1+\nu_1)/E_1 + (1-\nu_2)(1+\nu_2)/E_2}$ is the so-called Dundurs' parameter,[49] $P(x)$ and $Q(x)$ denote the normal and tangential tractions along the contact interface, respectively.

Equation (3) can be solved following a standard procedure of solving the inhomogeneous Hilbert equations.[9] Since the process is standard but rather tedious, the details are given in the Appendix A and neglected here. The solutions of Eq. (3) result in the following interfacial tractions in the contact region

$$\begin{cases} P(x) = -2\mathrm{Im}[I(x)] + \dfrac{E^*\beta}{2(1-\beta^2)}\varepsilon(x) \\ Q(x) = 2\mathrm{Re}[I(x)] + \dfrac{E^*x\beta}{2R(1-\beta^2)}, \end{cases} \tag{4}$$

where $I(x) = \frac{E^*(b+x)^{-\bar{r}}(a-x)^{-r}}{4\pi(1-\beta^2)}\left[\int_{-b}^{a}\left(-\varepsilon(t)-\frac{ti}{R}\right)\frac{(b+t)^{\bar{r}}(a-t)^{r}}{t-x}dt\right]$, $r=\frac{1}{2}+i\kappa$, and $\kappa=\frac{1}{2\pi}\ln\left(\frac{1+\beta}{1-\beta}\right)$, κ being the so-called oscillatory index. r is the stress singularity exponent near the contact edge, which is similar to the stress singularity of an interface crack in a bimaterial.

From Eq. (4), a set of stress intensity factors at the right and left contact edges are determined as

$$\begin{cases} K_{right} = -\sqrt{2\pi}\lim\limits_{x\to a}(a-x)^{r}[P(x)+iQ(x)] \\ K_{left} = -\sqrt{2\pi}\lim\limits_{x\to -b}(b+x)^{\bar{r}}[P(x)+iQ(x)], \end{cases} \tag{5}$$

with corresponding energy release rates

$$\begin{cases} G_{right} = \dfrac{1}{\cosh^2(\pi\kappa)}\dfrac{|K_{right}|^2}{2E^*} \\ G_{left} = \dfrac{1}{\cosh^2(\pi\kappa)}\dfrac{|K_{left}|^2}{2E^*}. \end{cases} \tag{6}$$

For the present study, it suffices to consider only the first order strain gradient. Taking $\varepsilon(x)=\varepsilon_A+\eta x$ (ε_A = strain at $x=0$ and η = strain gradient as shown in Fig. 2). Then, we have the normal and tangential tractions along the contact interface,

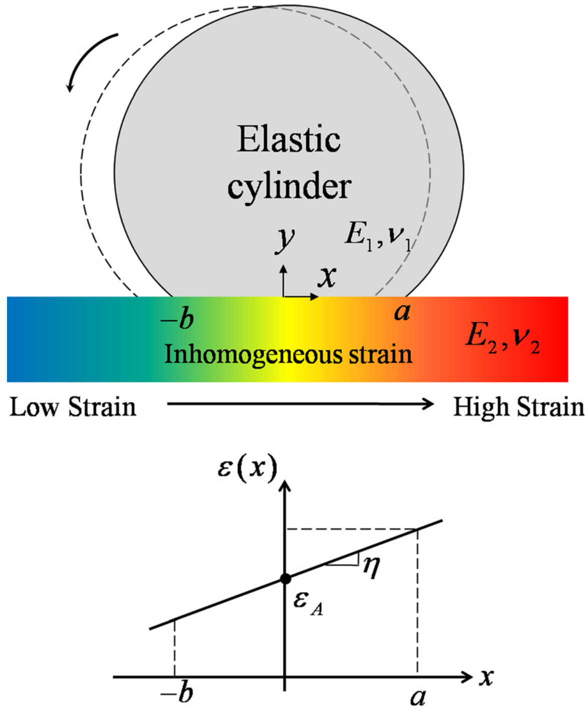

FIG. 2. Schematic of an elastic cylinder rolling on a substrate in the direction of strain gradient.

$$\begin{cases} P(x) = -2\mathrm{Im}[I(x)] + \dfrac{E^*\beta}{2(1-\beta^2)}(\varepsilon_A+\eta x) \\ Q(x) = 2\mathrm{Re}[I(x)] + \dfrac{E^*x\beta}{2R(1-\beta^2)}, \end{cases} \tag{7}$$

in which

$$I(x) = \frac{E^*}{4\pi(1-\beta^2)}\left[\begin{array}{l} -\varepsilon_A\left(\mathrm{i}(a+b)\kappa+\dfrac{a-b}{2}-x\right)\pi\,\mathrm{sech}(\pi\kappa)(b+x)^{-\bar{r}}(a-x)^{-r} \\ -\left(\eta+\dfrac{i}{R}\right)\pi\,\mathrm{sech}(\pi\kappa)\left[\begin{array}{l}\dfrac{(a+b)^2}{8}(1+4\kappa^2) \\ +\left(\mathrm{i}(a+b)\kappa+\dfrac{a-b}{2}\right)x-x^2\end{array}\right](b+x)^{-\bar{r}}(a-x)^{-r} \\ +\varepsilon_A\pi\mathrm{i}\tanh(\pi\kappa)+\left(\mathrm{i}\eta-\dfrac{1}{R}\right)x\pi\tanh(\pi\kappa) \end{array}\right]. \tag{8}$$

The energy release rates at the right and left contact edges are calculated as

$$\begin{cases} G_{right} = \dfrac{\pi E^*(a+b)}{16\cosh^4(\pi\kappa)(1-\beta^2)^2}\left\{\begin{array}{l}\left[2\kappa(\varepsilon_A+a\eta)+\dfrac{1}{R}\left(\dfrac{a+b}{4}(1+4\kappa^2)-a\right)\right]^2 \\ +\left[\eta\left(\dfrac{a+b}{4}(1+4\kappa^2)-a\right)-\varepsilon_A-\dfrac{2\kappa a}{R}\right]^2\end{array}\right\} \\ G_{left} = \dfrac{\pi E^*(a+b)}{16\cosh^4(\pi\kappa)(1-\beta^2)^2}\left\{\begin{array}{l}\left[2\kappa(\varepsilon_A-b\eta)+\dfrac{1}{R}\left(\dfrac{a+b}{4}(1+4\kappa^2)-b\right)\right]^2 \\ +\left[\eta\left(\dfrac{a+b}{4}(1+4\kappa^2)-b\right)+\varepsilon_A+\dfrac{2\kappa b}{R}\right]^2\end{array}\right\} \end{cases}. \tag{9}$$

For equilibrium, the net moment over the contact region should vanish, i.e.

$$M = \int_{-b}^{a} P(x)x dx = 0, \tag{10}$$

which yields a relation between a and b as

$$b = \left(\frac{3 - 2R\kappa\eta}{3 + 2R\kappa\eta}\right)a. \tag{11}$$

The contact region is symmetric ($b = a$) only in the absence of strain gradient, i.e., $\eta = 0$.

Comparing Figs. 1(a) and 1(b) yields the following relation;

$$a + b - [\bar{u}_{x1}(a) - \bar{u}_{x1}(-b)] = 2a_0, \tag{12}$$

where $\bar{u}_{x1}(a)$ and $\bar{u}_{x1}(-b)$ denote the surface displacements of the elastic cylinder at $x = a$ and $x = -b$ in the x-axis direction.

According to Ref. 48, the general expression of surface displacement of the elastic cylinder is

$$\bar{u}_{x1}(x) = -\frac{(1-2\nu_1)(1+\nu_1)}{2E_1}\left[\int_{-b}^{x} P(s)ds - \int_{x}^{a} P(s)ds\right] + \frac{2\left(1-\nu_1^2\right)}{\pi E_1}\int_{-b}^{a} Q(s)\ln|s-x|ds + C, \tag{13}$$

where C is a constant. Substituting Eq. (13) into (12) and combining Eqs. (7), (8), and (11) yield the contact lengths a and b. It is complex to find the analytical solutions of a and b, but numerical results can be achieved easily.

According to our experimental observation,[38] it can be inferred that the elastic cylinder in the present model will roll from right to left as shown in Fig. 2, which is consistent with the direction of strain gradient. The rolling process involves the detachment near the right trailing edge and attachment near the left leading edge. While the elastic cylinder does not sense the existing substrate strain at the leading edge as the cylinder rolls to attach to the substrate, the strain energy absorbed in the system due to the attachment equals in magnitude the energy released from the detachment behavior of a cylinder spontaneously adhering on a stress-free substrate. At the trailing edge, the strain energy will be released due to the detachment. Then, the resulting energy release rate due to a possibly initial rolling is

$$\begin{cases} G_{right} = \dfrac{\pi E^*(a+b)}{16\cosh^4(\pi\kappa)\left(1-\beta^2\right)^2}\left\{\begin{aligned} &\left[2\kappa(\varepsilon_A + a\eta) + \frac{1}{R}\left(\frac{a+b}{4}(1+4\kappa^2) - a\right)\right]^2 \\ &+\left[\eta\left(\frac{a+b}{4}(1+4\kappa^2) - a\right) - \varepsilon_A - \frac{2\kappa a}{R}\right]^2 \end{aligned}\right\} \\ G_{left}\Big|_{\substack{\varepsilon_A=0\\ \eta=0}} = \dfrac{\pi E^*}{16\cosh^4(\pi\kappa)\left(1-\beta^2\right)^2}\dfrac{a_0^3(4\kappa^2+1)^2}{2R^2} \end{cases}. \tag{14}$$

The criterion for the initiation of rolling is then written as

$$\left|G_{right} - G_{left}\Big|_{\substack{\varepsilon_A=0\\ \eta=0}}\right| \geq \Delta\Gamma, \quad \Delta\Gamma = \Delta\gamma_{trailing} - \Delta\gamma_{leading}, \tag{15}$$

where $\Delta\Gamma$ denotes the difference in work of adhesion at the two contact edges and $\Delta\gamma_{trailing}$ and $\Delta\gamma_{leading}$ are to be determined from the so-called "over-loading" and "under-loading" experiments.[50] The difference in work of adhesion, similar to a braking force, comes from the difference of separation and formation of the interface, which results from the unavoidable adhesion hysteresis or viscoelastic behavior of interfaces.[39,50,51] The difference in energy release rates at both contact edges in the present model looks like a driving force to overcome the difference in work of adhesion, i.e., the braking force. If the driving force is larger than the braking one, the cylinder in the present model will start to roll on the substrate. Such a phenomenon is quite similar to the case of a cylinder rolling on a flat rubber surface, in which the energy dissipated by hysteresis was considered as a resistance.[52]

Thus, the rolling criterion of the present model can be expressed as

$$\frac{\pi E^*(1+4\kappa^2)}{16\cosh^4(\pi\kappa)\left(1-\beta^2\right)^2}\left\{\begin{aligned} &\frac{\left[(a+b)^3 - 8a_0^3\right](1+4\kappa^2)}{16R^2} + \frac{a(a^2-b^2)}{2R^2} + \frac{(a+b)^2\kappa}{R}\varepsilon_A + (a+b)\varepsilon_A^2 \\ &+\frac{(3a-b)(a+b)}{2}\varepsilon_A\eta + \left[\frac{(a+b)^3}{16}(1+4\kappa^2) + \frac{a(a^2-b^2)}{2}\right]\eta^2 \end{aligned}\right\} \geq \Delta\Gamma. \tag{16}$$

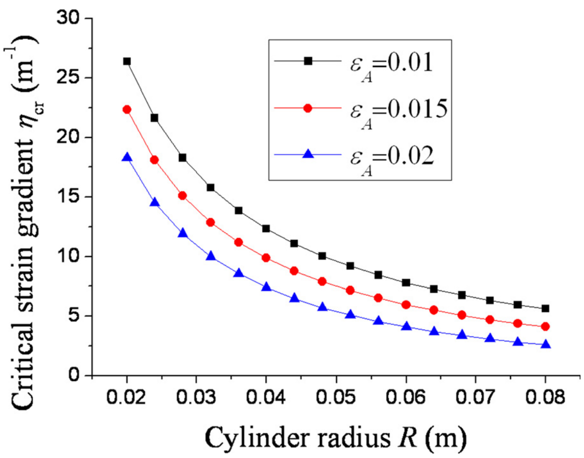

FIG. 3. The relation between the critical strain gradient for initial rolling and the cylinder radius at given strains at $x = 0$.

It indicates that the initial rolling of an elastic cylinder depends not only on the strain gradient but also on the strain in the substrate and the contact width. This result is consistent well with the prediction from the three-dimensional model of an elastic bubble adhering on an elastic substrate.[38] A critical strain gradient η_{cr} can be obtained from the relation $\left|G_{right} - G_{left}\big|_{\substack{\varepsilon_A=0\\ \eta=0}}\right| = \Delta\Gamma$ for a fixed strain ε_A at $x = 0$.

Figure 3 gives the critical strain gradient η_{cr} needed by the initial rolling as a function of the radius of the elastic cylinder when the strain at $x = 0$ is fixed. It shows that the critical strain gradient decreases with the increase of the cylinder radius for a determined strain at $x = 0$. For a given radius of the cylinder, the critical strain gradient decreases with an increasing strain at $x = 0$. Under a fixed critical strain gradient, the larger the cylinder, the smaller the strain ε_A at $x = 0$ is needed by the initial rolling. All these predictions are well consistent with not only the results found in the three-dimensionally spherical bubble experiment but also the solutions of the three-dimensionally theoretical model.[38]

III. CONCLUSIONS

In summary, a two-dimensionally adhesive contact model between an elastic cylinder and an elastic substrate subject to a graded strain is established, which is inspired by a recent experiment of spherical bubble rolling induced by graded strain in substrate. Closed-form solutions of interface tractions, energy release rates at the right and left contact edges are achieved. The criterion of initial rolling predicts that an elastic cylinder could roll on elastic substrates subject to a graded strain. The initial rolling of the elastic cylinder depends on not only the strain gradient but also the strain in the substrate and the initially free contact width. All these results suggest us to conduct rolling experiment of cylinders in the future. The phenomenon predicted experimentally and theoretically could provide a possible explanation for biological transports via muscle contractions.

ACKNOWLEDGMENTS

Support from the National Science Foundation of China (Grant Nos. 11372317 and 11125211), the 973 Nano-project (2012CB937500), and the CAS/SAFEA International Partnership Program for Creative Research Teams are gratefully acknowledged.

APPENDIX A: THE BASICS OF SOLUTION OF EQ. (3)

Rewrite Eq. (3) in a matrix form

$$\frac{1}{\pi}\int_{-b}^{a}\frac{\boldsymbol{A}}{s-x}\boldsymbol{f}(s)ds + \boldsymbol{B}\boldsymbol{f}(x) = \boldsymbol{C}, \tag{A1}$$

in which

$$\boldsymbol{f}(s) = \begin{bmatrix} Q(s) \\ P(s) \end{bmatrix}, \quad \boldsymbol{A} = \begin{bmatrix} 1 & 0 \\ 0 & 1 \end{bmatrix}, \quad \boldsymbol{B} = \begin{bmatrix} 0 & \beta \\ \beta & 0 \end{bmatrix} \quad \text{and} \quad \boldsymbol{C} = \begin{bmatrix} \dfrac{E^*\varepsilon(x)}{2} \\ -\dfrac{E^*x}{2R} \end{bmatrix}. \tag{A2}$$

In order to solve Eq. (A1), we define

$$F_k(z) = \frac{1}{2\pi i}\int_{-b}^{a}\frac{f_k(s)}{s-z}\mathbf{d}s, \quad k = 1, 2, \tag{A3}$$

in which $z = x + iy$ and $i = \sqrt{-1}$.

Then, we have

$$\begin{cases} f_k(x) = F_k^+(x) - F_k^-(x) \\ F_k^+(x) + F_k^-(x) = \dfrac{1}{\pi i}\displaystyle\int_{-b}^{a}\frac{f_k(s)}{s-x}\mathbf{d}s, \end{cases} \tag{A4}$$

where superscripts '+' and '−' stand for the limits of $F_k(z)$ as $y \to 0^+$ and $y \to 0^-$, respectively.

Thus, Eq. (A1) can be written as

$$\boldsymbol{U}\boldsymbol{F}^+(x) = \boldsymbol{V}\boldsymbol{F}^-(x) + \boldsymbol{C}, \tag{A5}$$

in which

$$\boldsymbol{U} = \boldsymbol{B} + i\boldsymbol{A}, \quad \boldsymbol{V} = \boldsymbol{B} - i\boldsymbol{A}. \tag{A6}$$

Before solving Eq. (A5), we first consider the eigenvalue problem

$$[\boldsymbol{U} - \lambda\boldsymbol{V}]\boldsymbol{W} = 0. \tag{A7}$$

Inserting Eqs. (A2) and (A6) into (A7) yields two eigenvalues

$$\lambda_1 = \frac{\beta-1}{\beta+1}, \quad \lambda_2 = \frac{\beta+1}{\beta-1}, \tag{A8}$$

and two normalized eigenvectors

$$\boldsymbol{W} = [\boldsymbol{W}_1\boldsymbol{W}_2], \tag{A9}$$

where

$$\boldsymbol{W}_1 = [1 \;\; i]^T, \quad \boldsymbol{W}_2 = [1 \; -i]^T. \tag{A10}$$

Introducing the following auxiliary functions

$$\boldsymbol{T}^{+} = \boldsymbol{W}^{-1}\boldsymbol{F}^{+}, \quad \boldsymbol{T}^{-} = \boldsymbol{W}^{-1}\boldsymbol{F}^{-}, \tag{A11}$$

and multiplying Eq. (A5) by $\boldsymbol{W}^{-1}$ leads to the decoupled equation

$$\boldsymbol{W}^{-1}\boldsymbol{U}\boldsymbol{W}\boldsymbol{W}^{-1}\boldsymbol{F}^{+} = \boldsymbol{W}^{-1}\boldsymbol{V}\boldsymbol{W}\boldsymbol{W}^{-1}\boldsymbol{F}^{-} + \boldsymbol{W}^{-1}\boldsymbol{C}, \tag{A12}$$

i.e.,

$$\boldsymbol{U}'\boldsymbol{T}^{+} = \boldsymbol{U}'\boldsymbol{T}^{-} + \boldsymbol{C}', \tag{A13}$$

in which

$$\boldsymbol{U}' = \boldsymbol{W}^{-1}\boldsymbol{U}\boldsymbol{W}, \quad \boldsymbol{V}' = \boldsymbol{W}^{-1}\boldsymbol{V}\boldsymbol{W}, \quad \boldsymbol{C}' = \boldsymbol{W}^{-1}\boldsymbol{C}.$$

Equation (A13) consists of two inhomogeneous Hilbert equations

$$\begin{cases} (1-\beta)T_1^{+} + (1+\beta)T_1^{-} = \dfrac{E^*}{4}\left[\dfrac{x}{R} - \varepsilon(x)i\right] \\ (1+\beta)T_2^{+} + (1-\beta)T_2^{-} = \dfrac{E^*}{4}\left[-\dfrac{x}{R} - \varepsilon(x)i\right] \end{cases}. \tag{A14}$$

The solutions to Eq. (A14) can be obtained following the standard procedure[53]

$$\begin{cases} T_1^{+} = \dfrac{-E^*i}{8(1-\beta)}\left(\varepsilon(x) + \dfrac{xi}{R}\right) - \dfrac{E^*(b+x)^{-\bar{r}}(a-x)^{-r}}{8\pi(1-\beta)}\left[\displaystyle\int_{-b}^{a}\left(\varepsilon(t) + \dfrac{ti}{R}\right)\dfrac{(b+t)^{-\bar{r}}(a-t)^{-r}}{t-x}dt\right] \\ \quad + c_1(b+x)^{-\bar{r}}(a-x)^{-r}e^{-\pi r i} \\ T_1^{-} = \dfrac{-E^*i}{8(1+\beta)}\left(\varepsilon(x) + \dfrac{xi}{R}\right) - \dfrac{E^*(b+x)^{-\bar{r}}(a-x)^{-r}e^{2\pi r i}}{8\pi(1-\beta)}\left[\displaystyle\int_{-b}^{a}\left(\varepsilon(t) + \dfrac{ti}{R}\right)\dfrac{(b+t)^{-\bar{r}}(a-t)^{-r}}{t-x}dt\right] \\ \quad + c_1(b+x)^{-\bar{r}}(a-x)^{-r}e^{\pi r i} \\ T_2^{+} = \dfrac{-E^*i}{8(1+\beta)}\left(\varepsilon(x) - \dfrac{xi}{R}\right) - \dfrac{E^*(b+x)^{-r}(a-x)^{-\bar{r}}}{8\pi(1+\beta)}\left[\displaystyle\int_{-b}^{a}\left(\varepsilon(t) - \dfrac{ti}{R}\right)\dfrac{(b+t)^{-r}(a-t)^{-\bar{r}}}{t-x}dt\right] \\ \quad + c_2(b+x)^{-r}(a-x)^{-\bar{r}}e^{-\pi\bar{r}i} \\ T_2^{-} = \dfrac{-E^*i}{8(1-\beta)}\left(\varepsilon(x) - \dfrac{xi}{R}\right) - \dfrac{E^*(b+x)^{-r}(a-x)^{-\bar{r}}e^{2\pi\bar{r}i}}{8\pi(1+\beta)}\left[\displaystyle\int_{-b}^{a}\left(\varepsilon(t) - \dfrac{ti}{R}\right)\dfrac{(b+t)^{-r}(a-t)^{-\bar{r}}}{t-x}dt\right] \\ \quad + c_2(b+x)^{-r}(a-x)^{-\bar{r}}e^{\pi\bar{r}i}. \end{cases} \tag{A15}$$

According to Eqs. (A2), (A4), and (A11), the interface tractions can be obtained from the following relations:

$$\begin{cases} P(x) = i(T_1^{+} - T_1^{-}) - i(T_2^{+} - T_2^{-}) \\ Q(x) = T_1^{+} - T_1^{-} + T_2^{+} - T_2^{-}. \end{cases} \tag{A16}$$

Substituting Eq. (A15) into (A16) yields

$$\begin{cases} P(x) = -2\mathrm{Im}[I(x)] + \dfrac{E^*\beta}{2(1-\beta^2)}\varepsilon(x) + \dfrac{2c_1(b+x)^{-\bar{r}}(a-x)^{-r}}{\sqrt{1-\beta^2}} - \dfrac{2c_2(b+x)^{-r}(a-x)^{-\bar{r}}}{\sqrt{1-\beta^2}} \\ Q(x) = 2\mathrm{Re}[I(x)] + \dfrac{E^*x\beta}{2R(1-\beta^2)} - \dfrac{2c_1(b+x)^{-\bar{r}}(a-x)^{-r}i}{\sqrt{1-\beta^2}} - \dfrac{2c_2(b+x)^{-r}(a-x)^{-\bar{r}}i}{\sqrt{1-\beta^2}}, \end{cases} \tag{A17}$$

in which

$$I(x) = \frac{E^*(b+x)^{-\bar{r}}(a-x)^{-r}}{4\pi(1-\beta^2)}\left[\int_{-b}^{a}\left(-\varepsilon(t) - \frac{ti}{R}\right)\frac{(b+t)^{\bar{r}}(a-t)^{r}}{t-x}dt\right]. \tag{A18}$$

The condition that both $P(x)$ and $Q(x)$ should be real requires

$$c_1 = -\bar{c}_2. \tag{A19}$$

The boundary condition

$$\int_{-b}^{a} [P(x) + iQ(x)]dx = 0 \tag{A20}$$

yields

$$c_1 = -\bar{c}_2 = 0. \tag{A21}$$

Then, we have

$$\begin{cases} P(x) = -2\mathrm{Im}[I(x)] + \dfrac{E^*\beta}{2(1-\beta^2)}\varepsilon(x) \\ Q(x) = 2\mathrm{Re}[I(x)] + \dfrac{E^* x\beta}{2R(1-\beta^2)}, \end{cases} \quad -b \le x \le a. \tag{4}$$

[1]K. L. Johnson, K. Kendall, and A. D. Roberts, Proc. R. Soc. London Ser. A **324**, 301 (1971).
[2]B. V. Derjaguin, V. M. Muller, and Y. P. Toporov, J. Colloid Interface Sci. **53**, 314 (1975).
[3]D. Maugis, J. Colloid Interface Sci. **150**, 243 (1992).
[4]D. Tabor, J. Colloid Interface Sci. **58**, 2 (1977).
[5]H. J. Gao and H. M. Yao, Proc. Natl. Acad. Sci. U.S.A. **101**, 7851 (2004).
[6]N. J. Glassmaker, A. Jagota, C. Y. Hui, and J. Kim, J. R. Soc. Interface **1**, 23 (2004).
[7]H. Yao and H. Gao, J. Mech. Phys. Solids **54**, 1120 (2006).
[8]Y. S. Chu, S. Dufour, J. P. Thiery, E. Perez, and F. Pincet, Phys. Rev. Lett. **94**, 028102 (2005).
[9]S. H. Chen and H. J. Gao, Proc. R. Soc. A **462**, 211 (2006).
[10]F. Jin and X. Guo, Int. J. Solids Struct. **49**, 2349 (2012).
[11]B. Alberts, D. Bray, J. Lewis, M. Raff, K. Roberts, and J. D. Watson, *Molecular biology of the cell*, 3rd ed. (Garland, New York, 1994), p. 949.
[12]G. Bao and S. Suresh, Nat. Mater. **2**, 715 (2003).
[13]H. J. Gao, W. D. Shi, and L. B. Freund, Proc. Natl. Acad. Sci. U.S.A. **102**, 9469 (2005).
[14]D. E. Ingber, J. Cell Sci. **104**, 613 (1993).
[15]N. Wang, J. P. Butler, and D. E. Ingber, Science **260**, 1124 (1993).
[16]P. R. Girard and R. M. Nerem, J. Cell. Physiol. **163**, 179 (1995).
[17]D. Choquet, D. P. Felsenfeld, and M. P. Sheetz, Cell **88**, 39 (1997).
[18]W. S. Haston, J. M. Shields, and P. C. Wilkinson, Expt. Cell Res. **146**, 117 (1983).
[19]C. G. Galbraith and M. P. Sheetz, Curr. Opin. Cell Biol. **10**, 566 (1998).
[20]S. Huang and D. E. Ingber, Nat. Cell Biol. **1**, E131 (1999).
[21]C. M. Lo, H. B. Wang, M. Dembo, and Y. L. Wang, Biophys. J. **79**, 144 (2000).
[22]B. Lorz, R. Simson, J. Nardi, and E. Sackmann, Europhys. Lett. **51**, 468 (2000).
[23]B. Geiger and A. Bershadsky, Cell **110**, 139 (2002).
[24]I. B. Bischofs and U. S. Schwarz, Proc. Natl. Acad. Sci. U.S.A. **100**, 9274 (2003).
[25]J. Y. Wong, A. Velasco, P. Rajagopalan, and Q. Pham, Langmuir **19**, 1908 (2003).
[26]S. A. Halbert, D. R. Becker, and S. E. Szal, Biol. Reprod. **40**, 1131 (1989).
[27]R. A. Lyons, E. Saridogan, and O. Djahanbakhch, Human Reprod. Update **12**, 363 (2006).
[28]S. Inan, G. Giray, H. S. Vatansever, K. Ozbilgina, N. K. Kuscub, and S. Sayhanc, Acta Histochem. **106**, 235 (2004).
[29]B. A. Lessey, "Integrins and uterine receptivity," in *Embryo Implantation: Molecular, Cellular and Clinical Aspects*, edited by D. D. Carson (Springer, New York, USA, 1999), pp. 210–222.
[30]J. T. Norwood, C. E. Hein, S. A. Halbert, and R. G. W. Anderson, Proc. Natl. Acad. Sci. U.S.A. **75**, 4413 (1978).
[31]S. P. Martinez, M. Viggiano, A. M. Franchi, M. B. Herrero, M. E. Ortiz, M. F. Gimeno, and M. Villalon, J. Reprod. Fertility **118**, 111 (2000).
[32]F. Arbab, J. Goldsby, N. Matijevic-Aleksic, G. X. Huang, K. H. Ruan, and J. C. Huang, Human Reprod. **17**, 3053 (2002).
[33]S. Kolle, S. Reese, and W. Kummer, Theriogenology **73**, 786 (2010).
[34]J. L. V. Shaw, S. K. Dey, H. O. D. Critchley, and A. W. Horne, Human Reprod. Update **16**, 432 (2010).
[35]S. Miyamoto, S. K. Akiyama, and K. M. Yamada, Science **267**, 883 (1995).
[36]M. C. Wodnicka and K. Burridge, J. Cell Biol. **133**, 1403 (1996).
[37]S. P. Palecek, Nature **388**, 210 (1997).
[38]L. Chen, S. H. Chen, and H. J. Gao, "Biomimetic study of rolling transport through smooth muscle contraction," Colloids and Surfaces B: Biointerfaces (unpublished).
[39]M. E. R. Shanahan, J. Adhesion **63**, 15 (1997).
[40]C. D. Bain, G. D. Burnetthall, and R. R. Montgomerie, Nature **372**, 414 (1994).
[41]F. Brochardwyart and P. G. Degennes, Comptes Rendus De L Acad. Des Sci. Ser. Ii Fascicule B **321**, 285 (1995).
[42]D. F. Dossantos and T. Ondarcuhu, Phys. Rev. Lett. **75**, 2972 (1995).
[43]M. E. R. Shanahan, J. Phys. D-Appl. Phys. **23**, 321 (1990).
[44]M. E. R. Shanahan and P. G. deGennes, Comptes Rendus De L Acad. Des Sci. Ser. Ii Fascicule B **324**, 261 (1997).
[45]M. E. R. Shanahan and K. Sefiane, Sci. Rep. **4**, 4727 (2014).
[46]I. N. Sneddon, Int. J. Eng. Sci. **3**, 47 (1965).
[47]M. Barquins, J. Adhesion **26**, 1 (1988).
[48]K. L. Johnson, *Contact Mechanics* (Cambridge University Press, Cambridge, 1985).
[49]J. Dundurs and D. B. Bogy, J. Appl. Mech. **36**, 650 (1969).
[50]A. D. Roberts and A. G. Thomas, Wear **33**, 45 (1975).
[51]M. E. R. Shanahan and F. Michel, Int. J. Adhesion Adhesives **11**, 170 (1991).
[52]J. A. Greenwood, H. Minshall, and D. Tabor, Proc. R. Soc. London A **259**, 480 (1961).
[53]G. F. Carrier, M. Krook, and C. E. Pearson, *Functions of a complex variable* (Hod Books, Ithaca, NY, 1983), p. 422.